Published in final edited form as:
J Am Chem Soc. 2011 March 2; 133(8): 2729–2741. doi:10.1021/ja1101085.

Fungal Indole Alkaloid Biosynthesis: Genetic and Biochemical Investigation of Tryptoquialanine Pathway in *Penicillium aethiopicum*

Xue Gao[1], **Yit-Heng Chooi**[1], **Brian D. Ames**[3], **Peng Wang**[1], **Christopher T. Walsh**[3], and **Yi Tang**[1,2,*]

[1]Department of Chemical and Biomolecular Engineering, University of California Los Angeles, 420 Westwood Plaza, Los Angeles, CA 90095.

[2]Department of Chemistry and Biochemistry, University of California Los Angeles, 420 Westwood Plaza, Los Angeles, CA 90095.

[3]Department of Biological Chemistry & Molecular Pharmacology, Harvard Medical School, 240 Longwood Avenue, Boston, MA 02115.

Abstract

Tremorgenic mycotoxins are a group of indole alkaloids which include the quinazoline-containing tryptoquivaline **2** that are capable of eliciting intermittent or sustained tremors in vertebrate animals. The biosynthesis of this group of bioactive compounds, which are characterized by an acetylated quinazoline ring connected to a 6-5-5 imidazoindolone ring system via a 5-membered spirolactone, has remained uncharacterized. Here, we report the identification of a gene cluster (*tqa*) from *P. aethiopicum* that is involved in the biosynthesis of tryptoquialanine **1**, which is structurally similar to **2**. The pathway has been confirmed to go through an intermediate common to the fumiquinazoline pathway, fumiquinazoline F, which originates from a fungal trimodular nonribosomal peptide synthetase (NRPS). By systematically inactivating every biosynthetic gene in the cluster, followed by isolation and characterization of the intermediates, we were able to establish the biosynthetic sequence of the pathway. An unusual oxidative opening of the pyrazinone ring by an FAD-dependent berberine bridge enzyme-like oxidoreductase has been proposed based on genetic knockout studies. Notably, a 2-aminoisobutyric acid (AIB)-utilizing NRPS module has been identified and reconstituted *in vitro*, along with two putative enzymes of unknown functions that are involved in the synthesis of the unnatural amino acid by genetic analysis. This work provides new genetic and biochemical insights into the biosynthesis of this group of fungal alkaloids, including the tremorgens related to **2**.

Keywords

mycotoxins; alkaloids; aminoisobutyrate; oxidoreductase

yitang@ucla.edu.

SUPPORTING INFORMATION AVAILABLE: Additional experimental procedures and compound characterizations. This material is available free of charge via the Internet at http://pubs.acs.org.

INTRODUCTION

Tremorgenic mycotoxins are a group of indole alkaloids that are capable of eliciting intermittent or sustained tremors in vertebrate animals by acting on the central nervous system (CNS).1 Grains, forages and animal feeds contaminated with the tremorgen-producing molds are one of the major sources of mycotoxin intoxications in cattle, sheep and dogs, where the clinical symptoms include diminished activity and immobility, followed by hyperexcitability, muscle tremor, ataxia, titanic seizures and convulsions.1,2 Based on their structural features, the tremorgenic agents can be divided into the indole-diterpenoids (e.g. penitrems and paspalitrems), the prenylated indole-diketopiperazines (e.g. fumitremorgens and verruculogens), and the quinazoline-containing indole alkaloids related to tryptoquivaline **2** (Scheme 1).[3,4] Tryptoquialanine **1** is highly similar to **2** and differs only in the alkyl substitution in the quinazoline ring. The mode of action of these tremorgens is not well understood, but they are thought to interfere with neurotransmitter release.[5–7] Some of the tremorgens also exhibit useful biological activities, for example, fumitremorgin C is a potent and specific inhibitor of breast cancer resistance protein (BCRP),[8] while the penitrems are shown to exhibit potent insecticidal activity.[9–11] Biosynthesis of the tremorgenic indole-diterpenoids and prenylated indole-diketopiperazines are currently subjects of intensive studies.[12–15] Comparatively, the biosynthesis of the tremorgenic quinazoline alkaloids related to **1** and **2** has not been elucidated.

The structurally related **1** and **2** are produced by several fungi in the *Penicillium* spp. and *Aspergillus clavatus*, respectively.[16–18] Both **1** and **2** are multicyclic compounds that exhibit structural features not observed among other indole alkaloids (Scheme 1). Common to both compounds is an acetylated quinazoline ring connected to a 6-5-5 imidazoindolone ring system via a 5-membered spirolactone. The imidazolidone ring is heavily modified, containing the N16 hydroxylamine and the C15 *gem*-dimethyl group. The structural difference between **1** and **2** is thought to arise from the incorporation of alanine or valine, respectively. The structures of **1** and **2** are also related to the pyrazino[*2,1-b*]quinazoline alkaloids such as fiscalin A **6** and fumiquinazoline A **7**.[19,20] These multicyclic scaffolds are assembled from various proteinogenic and nonproteinogenic amino acids by the actions of short nonribosomal peptide synthetase (NRPS) assembly lines[21,22]. Common building blocks shared by many compounds in this family are an anthranilic acid and a tryptophan.[16,23]

Recently, the anthranilate-activating adenylation (A) domains of several fungal NRPS have been characterized and the modular assimilation of the amino acids to synthesize **7** in *Aspergillus fumigatus* has been partially reconstituted in vitro.[23,24] The formation of the imidazoindolone moiety in **7** has been shown to involve a two-step oxidative-acylation of the indole ring by a single module NRPS and a flavin-dependent monooxygenase. A similar mechanism is likely involved in the biosynthesis of **1** and **2**, as well as other imidazoindolone-containing alkaloids, such as **9** and **10**.[25,26] Nevertheless, it is not known whether a pyrazinoquinazoline intermediate analogous to **7** is involved in the biosynthesis of **1** and **2**. Isolation of metabolites related to **2**, such as tryptoquivalone **3**, nortryptoquivaline **4** and deoxytryptoquivaline **5** have provided hints regarding possible biosynthetic intermediates and the origins of unique structural features.[16,27,28] For example, the isolation of **4** suggests that the *gem*-dimethyl group present in **2** may arise from the α-methylation of a monomethylated intermediate. However, to obtain a comprehensive understanding of the biosynthetic mechanisms of these complex fungal alkaloids, a combination of both genetic and biochemical approaches are needed, starting from the identification of the respective biosynthetic gene clusters.

Recently, we used 454 sequencing technology to gain partial genome information of *P. aethiopicum* and determined the gene clusters involved in biosynthesis of the aromatic polyketides viridicatumtoxin **11** and griseofulvin **12** (Scheme 2).[29] *P. aethiopicum* and *P. digitatum* have been reported previously to produce **1**; and a compound that has identical UV absorbance and mass to **1** were indeed detected by us in the extracts of *P. aethiopicum*. Therefore, the availability of the genome sequence data presented an excellent opportunity to study the biosynthesis of this family of fungal indole alkaloids. In this report, we present the identification and verification of the *tqa* gene cluster; functional assignment of the individual genes through genetic and biochemical approaches; and insights into the origins of the unique structural features of **1**.

RESULTS

Isolation of 1 and Verification of Structure

Compound **1** was isolated from a four-day culture of *P. aethiopicum* grown on YMEG medium at a final titer of 8 mg/L. Proton and carbon NMR spectra of the purified compound matched the previous published data (Table S3, Figure S6).[17] To verify the three dimensional structure of **1** as that shown in Scheme 1, especially that of the substituents on the imidazoindolone rings, **1** was crystallized from a methylene chloride/heptane mixture and the X-ray structure was solved as shown in Figure 1. All of the relative configurations of **1** matched that of the solved structures of **2** and **4**,[16,17,27] including positions C2, C3, C12 and C27. Notably, the *syn* stereochemical configuration across C2 and C3 of the indole ring is confirmed. The *R* configuration at position C12 is consistent with incorporation of a D-tryptophan moiety that likely arises through epimerization of L-tryptophan during NRPS assembly. The crystal structure is also consistent with the absolute configurations of **1** determined by NOE and of that of **4** from X-ray crystallography.[17,27]

Identification and Verification of Gene Cluster and Analysis

Having verified the structure of **1**, we scanned the sequenced genome of *P. aethiopicum* for possible gene clusters that are responsible for biosynthesis. The NRPS (AnaPS) from *Neosartorya fischeri* NRRL 181, which synthesizes acetylaszonalenin, has been previously identified.[30] Using the adenylation (A) domains of AnaPS, which activates an anthranilate and a tryptophan, the NRPS genes in *P. aethiopicum* were identified from the local genome database by TBLASTN program (Table S1). By eliminating the common NRPS genes (>89% identity) in *P. aethiopicum* and *P. chrysogenum*, the number of candidate NRPS genes was narrowed down from 16 to 10 (Table S1). Further bioinformatic analysis of functional domains along with a specific search of common NRPS homologs present in the genomes of both *P. aethiopicum* and the **2** producer *A. clavatus* NRRL1, led to the identification of a candidate trimodule NRPS on contig 1275 (PaeNRPS1275, 67% identity to ACLA017890) and a single module NRPS on contig 1022 (PaeNRPS1022, 64% identity to ACLA017900) (Figure 2A and Table 1). Sequence analysis of PaeNRPS1275 revealed high overall sequence identity (54%), and identical domain arrangement to the recently identified AFUA6G12080 (abbreviated as Af12080), which is proposed to synthesize fumiquinazoline F **14**, an intermediate on the way to fumiquinazoline A **7** (Table 1› Figure S7).24 The three A domains of PaeNRPS1275 are predicted to activate anthranillic acid, L-tryptophan, and L-alanine sequentially. The substrate specificity of the first A domain of Af12080, which activates anthranilic acid, has also been confirmed.[23] The presence of an epimerization domain (E) following the second module, which is proposed to activate L-tryptophan, is also consistent with the presence of D-tryptophan in the scaffold of **1**.

To verify the involvement of the PaeNRPS1275 NRPS in **1** biosynthesis, a double recombination cassette was constructed as shown in Figure 2B and transformed into

protoplasts of *P. aethiopicum*. Following selection of glufosinate and PCR verification, seventeen clones were identified to contain a Δ*tqaA* knockout (Figure S1). None of these clones produced **1** (Figure 2C) while the biosynthesis of other metabolites such as **11–13** were unaffected, confirming the essential role of PaeNRPS1275 (renamed as TqaA) in **1** biosynthesis. To eliminate the production of **12** and **13**, which are present at very high levels and can complicate detection and purification of compounds related to **1**, we constructed a Δ*gsfA* mutant of *P. aethiopicum* using the zeocin selection marker. The Δ*gsfA* strain was not longer able to synthesize **12** and **13** and is used in subsequent genetic analysis of the *tqa* cluster.

To complete the *tqa* gene cluster, a combination of fosmid sequencing and primer walking was performed to link different contigs with contig1275. The putative *tqa* gene cluster is shown in Figure 2A. To determine the putative boundary of the gene cluster, a comparative analysis with the sequenced *P. chrysogenum* genome was performed. Interestingly, the upstream *orf1-3* and downstream *orf7-9* flanking the *tqa* cluster are highly conserved and syntenic in *P. chrysogenum* (Table 1 and Figure 2A). We assumed that these conserved syntenic genes do not participate in biosynthesis of **1** but are involved in *Penicillium* housekeeping roles. Although *orf4* is not syntenic, it is highly similar to an ortholog in *P. chrysogenum* (96% identity, Table 1). The similarity of *orf5* and *orf6* to the possible orthologs in *P. chrysogenum* is significantly lower (37% and 25% identity respectively). To exclude the possible involvement of *orf4-6* in biosynthesis of **1**, single gene deletions were performed for these three genes on Δ*gsfA* background. As expected, production of **1** was unaffected in the Δ*orf4*, Δ*orf5* and Δ*orf6* mutants (Figure S2).

Based on the results from genetic knockouts and comparative genomic analysis, the *tqa* cluster embedded within the conserved syntenic regions is proposed to span ~32 kB and contains 13 genes (named *tqaA* – *tqaM*). The putative assignments of gene functions are shown in Table 1. The gene cluster encodes one transcriptional regulator TqaK. TqaK is a basic-region leucine zipper (bZIP) DNA-binding protein, and shared 27% protein identity with RadR, which regulates radicicol biosynthesis.[31] Deletion of *tqaK* using the *bar* selection marker did not completely abolish production of **1**, as observed for *radR*, but led to substantial attenuation of **1** titer to less than one-twentieth of the wild type strain (Figure 2C). This confirms the role of TqaK as a positive transcription regulator.

Functions of the two NRPSs in *tqa* gene cluster

The *tqa* gene cluster contains a monomodule (A-T-C) NRPS TqaB (PaeNRPS1022), which shares high sequence similarity to Af12050 that acylates L-alanine to the oxidized indole ring of **14** to yield **7**. The *tqa* gene cluster also contains two flavin-dependent oxidoreductases TqaH and TqaG, which are homologous to Af12060 and Af12070 found in the FQA gene cluster in *A. fumigatus*, respectively (Figure S3). While Af12060 is responsible for oxidation of the indole ring of **14** prior to *N*-acylation, Afl12070 is likely involved in the oxidative rearrangement of **7** towards other natural fumiquinazolines, such as fumiquinazoline C and D.[24] The presence of these enzymes, along with the similarity between TqaA and Af12080, hints that the biosynthesis of **1** may proceed first via the pyrazinoquinazolinone intermediate **14** and then the C2-epimer of **7**. Depending on the timing of the introduction of the C15-*gem*-dimethyl group, either 15-dimethyl-2-*epi*-fumiquinazoline A **18** or 2-*epi*-fumiquinazoline A **19** may be a biosynthetic precursor of **1**.

To identify these possible intermediates in the *tqa* pathway, we constructed single-gene knockouts of these three genes based on the Δ*gsfA* strain and analyzed the subsequent metabolite profiles (Figure 3A). Inactivation of TqaH led to the synthesis of a single metabolite at titers of 6 mg/L. The compound has the mass (*m/z* = 358) and UV absorption pattern consistent with that of **14**. Purification and NMR characterization confirmed the

compound is indeed **14** (Table S4), and points to the analogous role of TqaH in oxidizing **14** as previously demonstrated for Af12060 (Scheme 3).[24] The Δ*gsfA*/ Δ*tqaB* knockout strain no longer produced either **1** or **14**, but instead afforded a more polar metabolite with mass (*m/z* = 374). A possible structure of this compound is **15**, which might be the 2, 3-epoxidized version of **14** (Figure S8). This compound is highly unstable during purification and could not be isolated for further spectroscopic analysis. Finally, to probe the pathway shown in Scheme 3 and the role of TqaG as an enzyme that can possibly modify the fumiquinazoline-like intermediate, we analyzed the extract of Δ*gsfA*/Δ*tqaG*. This strain produced a predominant compound with mass (*m/z* = 459) and UV pattern suggestive of fumiquinazolines. This compound was purified and the structure was determined based on extensive NMR data to be that of **18** (Table S5, Figure S9). To verify the *syn* stereochemical configuration across C2 and C3 of the indole ring, as well the relative stereochemistry of other chiral carbons, the X-ray structure of **18** was determined and shown in Figure 3B.

More detailed examination of the Δ*gsfA*/Δ*tqaG* extract revealed the presence of another quinazoline compound (RT = 19.3 min) with mass (*m/z* = 445) corresponding to that of **18** with one fewer methyl group. The most likely candidate compound is therefore **19** in which the C15 position is occupied by a single methyl group which can be introduced from the side chain of L-alanine. Although this compound was present in a significantly lower titer, it was purified and thoroughly characterized by NMR to be indeed **19**. The loss of ^{1}H signal of the *gem*-dimethyl at δ=0.93 ppm and ^{13}C signal at δ=23.5 ppm, and the accompanying appearance of additional C<u>H</u> at δ=3.65 ppm and C29 methyl at δ=17.2 ppm, are consistent with the structural difference between **18** and **19** (Table S5, Figure S10).

Origin of *gem*-dimethyl Quaternary Carbon

The isolation of both **18** and as a minor component, **19**, from the Δ*gsfA*/ Δ*tqaG* strain provides clues to the timing and source of the *gem*-dimethyl incorporation. Since **18** is a relatively early intermediate in the pathway that leads to **1**, the *gem*-dimethyl can be introduced via one of the following different routes: a) activation of the nonproteinogenic amino acid 2-aminoisobutyrate (AIB) by TqaB; b) activation of L-alanine by TqaB and α-methylation while attached to the thiolation domain as an activated aminoacyl thioester; or c) direct α-methylation of **19** to yield **18**. The last alternative should be a difficult methylation reaction since generation of the nucleophilic enolate at C15 of **19** can be considerably more difficult for the amide carbonyl under biological settings.

To uncover the origin of the *gem*-dimethyl group, we first examined the A-domain specificity of TqaB. The uninterrupted *tqaB* was cloned by using splice-by-overlap extension PCR, expressed from *Escherichia coli* in both apo- and holo forms, and purified to single-band purity using Ni-NTA affinity chromatography (Figure 4A). ATP-[^{32}P]PP$_i$ exchange assay was used to monitor the activity of the A domain in the presence of different amino acids. As shown in Figure 4B, AIB is clearly the preferred substrate for adenylation by the A-domain of *apo* TqaB; while D-Ala, L-Ala, L-α-aminobutyric acid (AABA), and D-AABA also promoted exchange above background level (37, 27, 21, and 9% the level observed for AIB, respectively). Therefore, it is evident that compared to the functionally analogous Af12050 which does not activate AIB and only weakly activates D-Ala,[24] the A domain of TqaB has a clearly different substrate spectrum. The preference towards AIB hence strongly suggests that the *gem*-dimethyl in **1** and **18** is the result of AIB activation by TqaB.

To gain insight into the functional difference between the A domains of TqaB and Af12050, we aligned the 10-residue substrate specificity-determining sequence (10AA code) of the A domains, along with known L-Ala specific fungal A-domains (e.g. Af012050) and proposed AIB activating A domains of **2** (ACLA_017900) and that of peptaibol synthetases (Tex1

from *Trichoderma virens*) (Figure 4C).[32] The amino acid sequence of TqaB was submitted to the web-based NRPSpredictor and the 10AA code was extracted as DLFMMCGCIK.[33] ACLA_017900 shares the exactly same 10AA code as TqaB, which indicates that ACLA_017900 is likely to activate AIB as well. The 10AA code of Af12050 is highly similar between TqaB and ACLA_017900, but are different at position 3, 4 and 5. On the other hand, the 10AA code of TqaB A domain bears little similarity to AIB-activating domains in Tex1. Additional details with regard to how the 10AA code residues of TqaB and Af12050 may dictate their respective substrate specificities are provided in the discussion.

Having established that AIB is a likely building block of **1**, we next investigated the possible *tqa* enzymes that are involved in the synthesis of AIB. As with many NRPS clusters, the enzymes that are required for the synthesis of nonproteinogenic amino acids used by NRPS are typically encoded in the respective gene clusters.[34] These dedicated enzymes are therefore expressed only during the production of the nonribosomal peptides, which minimizes the interference of the products with ribosomal translational machinery. Since no AIB biosynthetic pathway is known to date and because none of the remaining *tqa* enzymes standout as potential candidates, we decided to generate single gene knockout strains of all remaining genes starting with the Δ*gsfA* strain. All of the *bar*-selected clones were verified by PCR to confirm the deletions; and were then cultured and extracted for metabolite analysis. The results of these knockout experiments are shown in Table 1.

From these studies, two genes with unknown functions were identified as likely to be involved in the biosynthesis of AIB. Knocking out of either *tqaM* or *tqaL* led to the production of the same shunt product **20** (*m/z* = 504), which matches the mass of, and is confirmed by NMR to be nortryptoquialanine (or tryptoquialanine B) (Figure 5A trace ii and trace iv, Table S3, Figure S11). Therefore, it appears these mutants are blocked in the synthesis of AIB, and TqaB instead selected L-alanine leading to the synthesis of **20**. Hence, the downstream enzymes that convert **18** to **1** are nonspecific towards the C15 *gem*-dimethyl. To prove that the Δ*tqaL* and Δ*tqaM* mutants are indeed blocked in AIB synthesis, we supplemented the mutant cultures with 1.5 mM AIB. As expected, production of **1** was restored to wild type levels in both mutants, thereby establishing TqaL and TqaM are essential for the *de novo* AIB synthesis in *P. aethiopicum* (Figure 5A trace iii and trace v).

To further prove AIB is involved in the biosynthesis of **1**, we aimed to reconstitute the conversion of **14** to **18** using an *E. coli* strain overexpressing TqaB and TqaH, and supplemented with AIB. The *tqaH* and *tqaB* cDNA were amplified with reverse-transcription (RT)-PCR and both genes were cloned into pCDFDuet™-1 vector for expression in BAP1.[35] After induction with IPTG and culturing overnight at 16°C, **14** was added to a final concentration of 120 μM and the culture was extracted with ethyl acetate after 2 hour. When TqaH was expressed alone, *in vivo* conversion of **14** to an oxidized product, likely **15**, was observed; along with a new compound that has mass consistent with a possible crosslinked dimer **30** (Figure 5B, Figure S19). Formation of the dimer was previously observed in the in vitro reaction containing **14** and Af12060, and our result here further verifies the function of TqaH as analogous to Af12060 (Scheme 3).[24] When both TqaB and TqaH were overexpressed in *E. coli*, along with supplementation with 1.5 mM AIB and **14**, complete oxidation followed by near complete acylation with AIB to yield **18** was observed. Excluding AIB led to the accumulation of **19**, further confirming the origin of the *gem*-dimethyl in **1**.

Tailoring Enzymatic Reactions Leading to Synthesis of 1

Analysis of the extract from the single gene knockout strains (in the background of Δ*gsfA*) shown in Table 1 also allowed us to assign functions to the remaining enzymes in the gene cluster, of which most are suggested to be involved in the conversion of **18** to **1** (Scheme 4).

The accumulation of **18** in the Δ*tqaG* knockout mutant suggests that TqaG is immediately involved in transforming **18** *en route* towards **1**. A BLAST search identified that TqaG has a FAD-binding site and belongs to the berberine bridge enzyme (BBE) superfamily. The BBE is proposed to initiate the oxidative cyclization of the *N*-methyl moiety of (*S*)-reticuline via the formation of a methylene iminium ion that undergoes subsequent ring closure to form the berberine bridge carbon, C-8, of (*S*)-scoulerine.[36] Therefore, we propose that TqaG might play a possible role in the 2-electron oxidation of the pyrazinone ring of **18** to yield the α-imine intermediate **21**. Hydrolysis of **21** yields the imino acid **22**, which can be rapidly converted to the ketone **23** upon nucleophilic attack by water at C27. Alternatively, the pyrazinone ring of **18** may be hydrolyzed to yield the C27 free amine, which can then be transaminated by a pyridoxal-5'-phosphate (PLP)-dependent enzyme to afford **23**. Several lines of reasoning however, make the second pathway unlikely: 1) no enzyme bearing resemblance to a possible transaminase is observed in the gene cluster; 2) hydrolysis of the highly stable pyrazinone ring without oxidation is difficult and should result in rapid recyclization to afford the starting compound **18**; and 3) the homolog of TqaG in the pathway of **7**, Af12070, has been proposed to initiate the intramolecular cyclization of **7** towards fumiquinazoline C and D via oxidation of the same carbon of the pyrazinone ring (B.D.A., C.T.W. unpublished results).

TqaI is similar to trypsin-like serine proteases present in insects (e.g. >30% identity to the homologs in the dust mite *Dermatophagoides farinae*).[37] A BLAST search using TqaI matched to only three fungal homologs (in *A. clavatus, A. terreus* and *Gibberella zeae*). The *tqaI* homolog in *A. clavatus* (ACLA_017930) is clustered together with the other *tqa* homologs in the genome, but absent in the gene cluster of **7** (Figure S3). Thus, it is likely that TqaI and ACLA 017930 play a common role in biosynthesis of **1** and **2** following formation of the pyrazinoquinazoline scaffold. From the Δ*gsfA*/Δ*tqaI* knockout strain, a compound (*m/z* = 476) that is most likely to be **23** was isolated (Figure S12). Upon purification of **23** by reverse-phase HPLC, the compound rapidly dehydrated to form the keto-lactone **24** (*m/z* =458). NMR characterization of **24** revealed the appearance of signals that correspond to an aliphatic ketone at δ=195.2 ppm (Table S6, Figure S14). Thorough 2D NMR confirmed the structure of **24** to be that of deoxynortryptoquialanone, in which the bridging spirolactone is installed. These evidences therefore suggest that TqaI is likely an accessory enzyme in the enzymatic lactonization of **23** to produce **24**, a reaction that may also proceed spontaneously. Indeed, the Δ*gsfA*/Δ*tqaI* strain continued to produce **1** as shown in Figure 5; and the combined level of **23** and **1** in this strain is near the titer of **1** in the wild type strain.

TqaE belongs to class A flavoprotein monooxygenases and shares moderate similarity to the characterized TqaH (39% identity) and Af12060 (35% identity). Recently, a pair of TqaE/TqaH homologs (NotB/NotI) were identified in the notoamide gene cluster (both shared 45% identity to TqaE), which were proposed to catalyze a 2,3-epoxidation and a *N*-hydroxylation of the tryptophan-derived indole ring to form the final notoamide A.[15] Indeed, deoxynortryptoquialanone **24** was also isolated from the Δ*gsfA*/Δ*tqaE* strain together with a tryptoquialanine-like compound **28** (*m/z* = 502). Compared to that of **1**, the NMR signals of **28** are nearly identical but with the loss of the *N*-hydroxyl signal at δ = 7.95 ppm and appearance of a new NH signal at δ = 3.18 ppm (Table S7, Figure S17). Based on the NMR information, **28** is assigned to be deoxytryptoquialanine as shown in Scheme 4. The isolation of **24** and **28** are consistent with the predicted *N*-hydroxylation function of TqaE. While the

exact timing of the hydroxylamine formation is not known, isolation of the ketone **24** suggests that *N*-oxidation of **24** to **25** may take place immediately following spirolactone formation. The high titer of **28** also indicates that the remaining tailoring steps in the *tqa* pathway can function in the absence of *N*-hydroxylation.

Formation of **1** from **25** requires the stereospecific reduction and acetylation of the C27 ketone. The most likely enzyme candidate in the *tqa* gene cluster for the ketoreduction is TqaC, which is homologous to putative NADPH-dependent short chain dehydrogenases. Inactivation of TqaC should therefore lead to accumulation of **25** in the culture extract. As expected, the Δ*gsfA*/Δ*tqaC* strain produced a single shunt product with mass (*m/z* = 474) and NMR data consistent with that of tryptoquialanone **25** (Figure 6, Table S6). Interestingly, 27-*epi*-isomers of **2** and **4** have been isolated from *Corynascus setosus.*[38,39] Based on the deduced biosynthetic pathway of **1** and the role of TqaC, the stereochemical difference at position C27 between **2/4**, and the corresponding epimers can be attributable to the different stereospecificity of the ketoreductase *tqaC* homologs in *A. clavatus* (ACLA_061530) and in *C. setosus*.

Finally, in the Δ*gsfA*/Δ*tqaD* strain in which putative acetyltransferase TqaD is inactivated, two metabolites **26** and **27** that have masses (*m/z* = 476) consistent with the TqaC-catalyzed ketoreduction of **25** were observed (Figures S15 and S16). **26** and **27** existed in equilibrium during extraction and purification, which prevented NMR characterization of individual compounds. However, this equilibrium is expected for a C27-reduced and unacetylated intermediate, as the interconversion between the spirolactone **26** (γ-lactone) and the oxazinoquinazoline **27** (δ-lactone) should take place readily under aqueous conditions. To examine the acetyltransfer reaction in more detail, we overexpressed and purified the hexahistidine tagged TqaD from BL21 (DE3). When incubated with a mixture of **26** and **27** purified from Δ*gsfA*/Δ*tqaD* and acetyl-CoA, formation of **1** was readily observed (Figure S4). Similarly when incubated with **1** and assayed for the reverse hydrolysis reaction with 20 μM TqaD, we were able to detect the formation of both **26** and **27.** In both assays, we also observed the formation of a new compound **29** that has the mass (*m/z* = 494) corresponding to the ring opened form of **26** and **27** (Figure S18). When extracted under strong acid conditions (5% TFA), **29** can be nearly completely lactonized into **26** and **27.** Acetylation of **26** by TqaD to yield **1** is therefore the last step in the *tqa* pathway and is critical to prevent opening of the connecting spirolactone ring.

The only remaining gene that has not been assigned a putative function is *tqaF*, which encodes an enzyme belonging to the haloacid dehalogenase superfamily. The Δ*gsfA*/Δ*tqaF* strain continued to synthesize **1** at the same level as the wild type, which indicates that this enzyme may not be essential in the proposed pathway.

DISCUSSION

In work reported in this paper, we have identified a gene cluster from *P. aethiopicum* that is involved in the biosynthesis of the tremorgenic mycotoxin tryptoquialanine **1**. The chemical logic and enzymatic machinery for generation of the architecturally complex tryptoquialanine peptidyl alkaloid scaffold from simple building blocks is revealed. By systematically inactivating every gene (15 genes total, except the transporter-encoding *tqaJ*) in the cluster, followed by isolation and characterization of the intermediates, we were able to establish the enzymatic sequence of the pathway. Four amino acids, two of them nonproteinogenic (anthranilate, AIB), are utilized by two nonribosomal peptide synthetase enzymes (TqaA and TqaB) that between them contain four modules, one for each building block activated and incorporated in an identical fashion to that of the pyrazinoquinazoline **7**. Notably, an AIB-utilizing NRPS module (TqaB) has been reconstituted *in vivo*, along with

identification of two putative enzymes (TqaM and TqaL) of unknown functions that are involved in the synthesis of this unnatural amino acid. The oxidative annulation of the AIB moiety onto the indole ring derived from the tryptophan building block is a particularly intriguing synthetic sequence.

P. aethiopicum is closely related to the penicillin-producing *P. chrysogenum*, whose genome has been sequenced,[40] but both species produce distinct secondary metabolites.[18] As one of the demonstrations, we previously showed that comparative genomics can be a useful tool to narrow down the biosynthetic genes responsible for production of a particular metabolite by exclusion of orthologous genes.[29] The structural similarities between **1** and **2** suggest that homologous genes are likely involved in their biosynthesis. Using a similar strategy coupled with a genome-wide search of common NRPSs in *P. aethiopicum* and *A. clavatus*,[41] which produces **2**, we were able to pinpoint the trimodular NRPS TqaA and single module NRPS TqaB, and subsequently confirm their involvement in biosynthesis of **1** by targeted gene deletion. The observation of conserved syntenic regions flanking the *tqa* gene cluster when compared to the corresponding genetic locus in *P. chrysogenum*, is akin to the *vrt* and *gsf* loci in the previous study.[29]

The corresponding *tqa* homologs in the *A. clavatus* genome that are predicted to be involved in the biosynthesis of **2** were identified via BLAST search (Table 1, Figure S3). As in *tqa* cluster, the corresponding homologs for *tqaA, tqaB, tqaE, tqaG, tqaH*, and *tqaI* are clustered in the *A. clavatus* genome. Interestingly, there are several genes in the putative *tqv* cluster for **2** that are not clustered together with the NRPS genes but fall on a separate genomic scaffold. Specifically, the homologs for the ketoreductase (*tqvC*) and acetyltransferase (*tqvD*) are adjacent to each other and fall on the genomic scaffold 1099423829796. The corresponding *A. clavatus* homologs for *tqaL* and *tqaM* are also located next to each other on the same genomic scaffold as *tqvC* and *tqvD*, but the two pairs are located 440 kbp apart. Similar fragmentation of secondary metabolic gene clusters has also been observed in the pathway for dothistromin, a mycotoxin that is structurally similar to the aflatoxin intermediate versicolorin A.[42] The presence of repeating sequences in the *tqa* gene cluster may suggest recent recombination or horizontal gene transfer events, which brought the genes in the *tqa* pathway into proximity. The clustering of *tqa* genes in the *P. aethiopicum* genome therefore presents an excellent opportunity to study the function of individual genes in the pathway.

Initial examination of the peptide linkages in **1** suggested that the amino acids may be assembled in the order of alanine or pyruvic acid, anthranilic acid and tryptophan, followed by the lactonization and release of the tripeptide from a trimodule NRPS. *N*-acylation of the indole ring with alanine/AIB could follow thereafter. However, the identification of TqaA as a trimodular NRPS with shared domain architecture and sequence similarity to Af12080 that synthesizes **14** (Figure S3), strongly indicates that **14** could be a common intermediate for both pathways. The knockout of *tqaH* confirmed that **14** is indeed the common intermediate and the formation of the spirolactone in **1** therefore requires opening of the pyrazinone ring, which partially masked the biosynthetic origin of **1**. Furthermore, identification of **14** as the authentic intermediate demonstrated that the TqaA trimodular NRPS utilizes L-Ala instead of pyruvic acid. Other homologous genes shared by the two gene clusters are the *tqaB, tqaH* and *tqaG*. From the corresponding knockout studies, the roles of TqaB and TqaH are indeed consistent with those corresponding homologs involved in the synthesis and tailoring of **7**. The isolation of **18** from Δ*gsfA*/ Δ*tqaG* mutant suggests that TqaG is the immediate oxidative tailoring enzyme in the pathway. The intriguing stereochemical difference between **18** and **7** across the C2 and C3 positions of the indole ring may be attributed to the functional difference between TqaB and Af12050. Whereas **7** contains the *anti* configuration that would be expected from epoxide opening by the free amine group of alanine, the *syn*

addition in **18** points to a mechanism in which the 3-hydroxyiminium cation **16** is the true intermediate for nucleophilic attack of the TqaB-activated α-amino group on the iminium ion to yield **17** (Scheme 3). The nucleophilic nitrogen on the dearomatized indole ring presumably then attacks the aminoacyl-TqaB thioester to form the 6-5-5 imidazoindolone scaffold.

By a combination of genetic and biochemical means, we determined the *gem*-dimethyl moiety in **1** is incorporated via the activation of the unnatural amino acid AIB by the monomodular NRPS TqaB. Gene deletion of *tqaM* and *tqaL* abolished the production of AIB, and TqaB instead activated L-Ala to produce **20**. We therefore propose that TqaM and TqaL are responsible for the production of AIB in *tqa* gene cluster. Although AIB is a commonly found amino acid constituent of many fungal secondary metabolites, the enzymatic basis for its biosynthesis is not known. BLAST search of the GenBank database using the amino acid sequences of TqaM and TqaL showed that homologs of these two enzymes can be found in other fungal genomes, and in most cases, adjacent to each other. These include ACLA_063360 and ACLA_063370 in *A. clavatus*, NCU01071 and NCU01072 in *Neurospora crassa* OR74A and SMAC_03146 and SMAC_03147 in *Sordaria macrospora*. AIB is most well-known for its abundant incorporation into a class of linear antimicrobial peptides named peptaibols (peptaibiotics), characterized prominently by high proportion of α,α-dialkylated amino acids.[32,43] The membrane-modifying properties of peptaibols and their ability to form transmembrane voltage-dependent channels have attracted much interest.[44,45] Since the peptaibol synthetase Tex1 homolog has been found in the sequenced *Trichoderma reesei* genome,[46,47] we searched the JGI *T. reesei* v2.0 database for TqaM/L homologs. Indeed, e_gw1.17.140.1 and e_gw1.19.93.1 were identified as homologs for TqaM and TqaL respectively. However unlike in the other fungal genomes, the two homologs in *T. reesei* fall on different genomic scaffolds (Figure S3). The presence of TqaM and TqaL homologs in other fungal genomes maybe indicative of their undiscovered capability to produce AIB, and thus can be a useful tool for genome mining of the antimicrobial peptaibols and other AIB-containing secondary metabolites.

TqaM was predicted to have a conserved Class II aldolase domain with a Zn^{2+} binding site. The closest homolog of TqaM is NCU01071, which shares homology to NovR/CloR (40% and 39% identity, respectively) from the novobiocin/clorobiocin biosynthesis pathway.[48] CloR has been verified to be a bifunctional non-heme iron oxygenase.[49] Although a conserved DUF2257 domain was found among the TqaL and similar proteins, the function of this conserved domain is not known. Raap et al.[50] reported that 2,2-dialkylglycine decarboxylase (DGD) is capable of converting AIB to acetone, and hence the PLP-dependent enzyme was also proposed to catalyze the reverse reaction, where AIB is synthesizes from acetone and CO_2.[46] Another possible biosynthetic mechanism might be modification of alanine with a PLP-dependent enzyme to generate the α-carbanionic species to attack the electrophilic methyl group of *S*-adenosylmethionine. However, neither TqaM nor TqaL contain the required PLP or SAM (*S*-adenosylmethionine) binding domains. Therefore, the functions of TqaM and TqaL cannot be predicted at this point and is the subject of further investigations. It is also to be determined if TqaM/L homologs are involved in biosynthesis of other α,α-dialkylated amino acids, such as isovaline (IVA).

Homology modeling and analysis of the putative substrate binding pockets of the TqaB and Af12050 A-domains provides a means to rationalize the observed differences in substrate specificities (Figure S5). The key change appears to be at position 4 (Pos4) of the 10 AA code, in which the bulkier methionine in TqaB is modeled to favorably contact both the Pos2 Leu and the *pro-R* methyl of 2-AIB. In Af12050 the Pos4 residue is changed to valine. The shorter side chain length of Val compared to Met allows for an alternate conformation of the Pos2 Leu, in this conformation the side chain would make favorable contacts with L-

Ala but clash with the *pro-R* methyl group of 2-AIB, therefore resulting in the preferential binding and activation of L-Ala in the biosynthesis of **7**. However, the 10AA code of TqaB-A domain shares low similarities to the proposed AIB activation A domains in Tex1, which suggests that the AIB-activating A domains in TqaB/TqvB and those in other peptaibol synthetases, such as ampullosporin synthetase,[51] and alamethicin synthetase,[52] may have evolved separately.

The conversion of the tricyclic fumiquinazoline F **14** scaffold to the bicyclic framework in the tremorgens **1** and **2** with installation of the γ-spirolactone is an intriguing set of chemical transformations. The scaffold of **14** is first elaborated to an epimer of **7** in an annulation of the indole ring derived from tryptophan. The annulation can use L-alanyl thioester linked to the pantetheinyl arm of the NRPS protein TqaB to produce **19**, but TqaB prefers the unusual AIB yielding **18**. This imidazolindolone-containing intermediate is then subjected to a series of steps which take apart the pyrazinone ring of the tricyclic quinazoline framework. It appears that the process starts with oxidation of the secondary amine to the imine and that the C27-N10 bond is then fragmented in an unusual manner to yield formally the imine and acid components. The imine can hydrolyze to the ketone, observed as an intermediate **24**. *N*-hydroxylation requires opening of the pyrazinone ring since no *N*16-hydroxylated pyrozinoquinazoline intermediate was obtained. Reduction of the ketone **25** to alcohol **26** then sets up the possibility of an equilibrium between the dihydroxy acid, the spiro-γ-lactone, and the δ-lactone, all of which are detectable in specific knockout mutants. Regioselective acetylation of the C27-OH by the acetyltransferase TqaD fixes the final product **1** with the γ-lactone ring. Whether the ring-opening of the oxidized pyrazine ring in **21** from TqaG action is by net hydrolysis or involves intramolecular capture of **21** by the OH at C3 of the imidazoindolone moiety to yield **24** directly is not yet known but would provide a driving force for fragmentation of **21**. Note that the nucleophilic-OH for spirolactone formation in **25** was introduced by oxidation/annulation of the indole side chain that happened at the stage of annulation of **14**. Conversion of **18** to **26** with a dramatically rearranged molecular architecture occurs by cryptic redox processes: regiospecific oxidation of the secondary amine in the quinazoline framework of **18** and then rereduction of the carbonyl after imine hydrolysis and spirolactone formation.

Given the remarkable morphing of the fumiquinazoline F scaffold **14** to the rearranged framework of the tryptoquialanine scaffold **1** with the above annulation and also γ-spirolactone formation, the pathway is remarkably short and efficient. Four redox enzymes are called into play: three of them (TqaH,G,E, acting in that order) contain FAD, the other (TqaC) utilizes NADPH in a conventional ketone to alcohol reduction of **25** to **26**. The flavoenzymes were proposed to carry out epoxidation of the indole side chain in 14 (TqaH), oxidation of the secondary amine linkage to cyclic imine in the pyrazinone ring of the pyrazinoquinazoline(TqaG) as the initiating step in fragmentation, and N-hydroxylation of the imidazoindolone (TqaE: 24 to 25), respectively. These transformations underscore the versatility of the FAD coenzyme for a wide chemical range of redox transformations by these biosynthetic enzymes. The detailed mechanisms of these novel enzymatic reactions are currently under investigation.

MATERIALS AND METHODS

Materials

P. aethiopicum, IBT 5753, was obtained from the IBT culture collection (Kgs. Lyngby, Denmark). All other chemicals and solvents were purchased from either Sigma-Aldrich or Fisher Scientific unless otherwise noted.

Spectroscopic Analysis

The NMR identification of compounds was performed on a Bruker ARX500 at the University of California Los Angeles Department of Chemistry and Biochemistry NMR facility. LC/MS spectra were obtained on a Shimadzu 2010 EV liquid chromatography mass spectrometer using positive and negative electrospray ionization and a Phenomenex Luna 5 μm, 2.0 mm × 100 mm C18 reverse-phase column. Samples were separated on a linear gradient of 5 to 95% CH_3CN in water (0.1% formic acid) for 30 min at a flow rate of 0.1 mL/min followed by isocratic 95% CH_3CN in water (0.1% formic acid) for another 15 min.

Bioinformatic Analysis

The 454-generated partial genomic sequencing data of *P. aethiopicum* is the same version as previously published,[29] and was formatted into a local database for BLAST searches. Gene predictions were performed using the FGENESH online server (Softberry) and manually checked by comparing with homologous gene/proteins in the GenBank database. Functional domains in the translated protein sequences were predicted using Conserved Domain Search (NCBI). The amino acid sequences of TqaB and other NRPS adenylation domains were submitted to NRPSpredictor for automated extraction of specificity-defining residues as the 10AA code.[33] The sequence of the *tqa* gene cluster has been submitted to GenBank with the accession number HQ591508.

X-ray Crystallographic Analysis

1 was crystallized from a mixture of methylene chloride/heptanes and **18** was obtained from the acetone/methanol mixture. X-ray diffraction was performed by the University of California Department of Chemistry and Biochemistry crystallography facility. Additional details can be found in the supplementary methods. The crystal structures of **1** and **18** are deposited at the Cambridge Crystallographic Data Centre and allocated the deposition numbers CCDC 800378 and 800379, respectively.

Construction and Screening of Fosmid Library

Fosmid library of *P. aethiopicum* was constructed using the CopyControl™ Fosmid Library Production Kit (Epicentre Biotechnologies, Madison, WI) following the manufacturer's instruction. Screening by direct colony PCR was carried out using GoTaq polymerase (Promega, Madison, WI). Initial screening was performed using pools of ~200 colonies and narrowed down to single colonies. Positive clones identified were sent for fosmid end-sequencing and primer walking. Adjacent contigs were identified from the *P. aethiopicum* genomic database using local BLAST search of the partial fosmid sequences and assembled by pairwise alignment.

Fungal Transformation and Gene Disruption in *P. aethiopicum*

Polyethylene glycolmediated transformation of *P. aethiopicum* was performed essentially as described previously.[29] The homologous regions flanking the resistant marker were increased to ~2 kb and other steps for construction of fusion PCR knockout cassettes containing the *bar* or *zeocin* gene were performed as described elsewhere.[53] Fusion PCR products were sequenced before using for transformation. ~7 μg DNA was gel-purified for each transformation. The *bar* gene with the *trpC* promoter was amplified from the plasmid pBARKS154,[55], which was obtained from the Fungal Genetics Stock Center (FGSC). The zeocin gene with the *gpda* promoter was amplified from the plasmid pAN8-1 (a gift from P. J. Punt, Institute Biology Leiden).[56] Glufosinate used for the selection of *bar* transformants was prepared as described previously.[29] Miniprep genomic DNA from *P. aethiopicum* transformants was used for PCR screening of gene deletants and was prepared as described elsewhere for *A. nidulans*.[57] Primers used for amplification of fusion PCR products and

screening of transformants, are listed in Table S2. Approximately 50 glufosinate-/zeocin-resistant transformants were picked and screened with PCR using a bar/zeocin gene primer and primers outside of the deletion cassette.

Chemical Analysis and Compound Isolation

For small-scale analysis, the *P. aethiopicum* wild-type and transformants were grown in stationary YMEG liquid culture (4 g/l yeast extract, 10 g/l malt extract, 5 g/l glucose and 16 g/l agar) for 4 days at 25°C. The cultures were extracted with equal volume of ethyl acetate and evaporated to dryness. The dried extracts were dissolved in methanol for LC-MS analysis. For large-scale analysis, the ethyl acetate (EA) extract from a two liters stationary liquid culture of each mutant was evaporated to dryness and partition between EA/H_2O twice. After evaporation of the organic phase, the crude extracts were separated by silica chromatography. The purity of each compound was checked by LC-MS and the structure was confirmed by NMR.

Expression and Purification of Recombinant Enzymes

TqaB and TqaD cDNA were cloned into a pET28 vector with an *N*-terminal hexahistidine tag and expressed in *E. coli* BL21(DE3) strain. The transformant was cultured in 500 mL LB medium containing 35 mg/L kanamycin at 37°C to optical density (OD600) value of 0.4~0.6. Protein expression was induced with 0.1 mM IPTG and the subsequent expression was performed at 16°C overnight. Cells were collected by centrifugation (2000 g, 4°C, 15 min), resuspended in 30 ml Buffer A (50 mM Tris–HCl, pH 8.0, 2 mM DTT, 2 mM EDTA), and lysed by sonication. Cell debris and insoluble proteins were removed by centrifugation (20,000 g, 4°C, 1 hr). To the cleared cell lysate, excess amount (0.5 ml) of Ni-NTA resin (QIAGEN, Valencia, CA) was added to each sample. The TqaB protein was then purified using a step gradient of Buffer A with increasing concentration of imidazole (10 and 20 mM) and was eluted with 5 mL Buffer A containing 250 mM imidazole. Protein purity was qualitatively assessed by SDS-PAGE and concentration was quantitatively determined by the Bradford protein assay using bovine serum albumin as the standard.

ATP-[^{32}P]PP_i exchange assay for TqaB

Reactions (100 μL) contained 2 mM ATP, 2 mM $MgCl_2$, 3 mM Na_4[^{32}P]PPi (0.2 μCi), 2 μM TqaB, and 2 mM amino acid substrate in buffer (50 mM Tris-HCl (pH7.5), 100 mM NaCl, 5mM TCEP, and 5% glycerol). Enzyme was added last to initiate the reactions and, following a 60 min incubation at 25 °C, the reactions were stopped by adding 400 μL of a quench solution (1.6% (w/v) activated charcoal, 100 mM sodium pyrophosphate, and 3.5% perchloric acid in water). The charcoal was collected by centrifugation, washed twice with quench solution minus charcoal, and the absorbed radioactivity detected by liquid scintillation counting.

E. coli Mediated Biotransformation of 14 to 18

TqaH cDNA was amplified by RT-PCR using M-MLV reverse transcriptase (Promega) and AccuPrime™ Pfx DNA polymerase (Invitrogen, Carlsbad, CA); and was cloned into pCDFDuet™-1 (EMD Chemicals, Gibbstown, NJ) and transformed into *E. coli* BAP1 strain[35]. The transformant with the TqaB and TqaH dual-expression plasmid was grown in LB medium at 37 °C to an OD600 of 0.4–0.6, at which time the cultures were cooled to 16 °C, and then induced with 0.1 mM IPTG at 250 rpm and grown at 16°C for overnight. To increase cell density, the *E. coli* cells were concentrated 10-fold before addition of substrates. A 10 mL aliquot of each culture was collected by centrifugation (4 °C, 2000 g, 10 min). The cell pellet was gently resuspended in 1 mL of medium supernatant, followed by addition of 6 μL **14** (20 mM stock) to a final concentration of 120 μM. The small cultures

were then shaken at 300 rpm at 25 °C for 2 hrs. For product detection, 100 μL of cell culture was collected and extracted with 500 μL of ethyl acetate. The organic phase was separated, evaporated to dryness, redissolved in methanol, and then subjected to LC-MS analysis.

Supplementary Material

Refer to Web version on PubMed Central for supplementary material.

Acknowledgments

This work is supported by NIH Grant 1R01GM092217 to Y. T.; 1F32GM090475 to B. D. A.; and 1R01GM49338 to C. T. W. We thank Prof. Neil Garg for helpful discussions and Prof. Peter J. Punt for the generous gift of the plasmid pAN8-1. We thank Wei Xu for advice on compound crystallization. We thank Dr. Saeed I. Khan at University of California Department of Chemistry and Biochemistry crystallography facility for solving the X-ray structures. Ian McRae is thanked for his help as an undergraduate research assistant.

REFERENCES

1. Cole RJ. J. Food Prot 1981;44:715.
2. Evans, T.; Gupta, R. Veterinary toxicology: basic and clinical principles. Gupta, R., editor. New York: Academic Press; 2007. p. 1004
3. Steyn P, R V. Fortschr. Chem. Org. Naturst 1985;48:1. [PubMed: 3912307]
4. D' Yakonov A, Telezhenetskaya M. Chem. Nat. Compd 1997;33:221.
5. Knaus HG, McManus OB, Lee SH, Schmalhofer WA, Garciacalvo M, Helms LMH, Sanchez M, Giangiacomo K, Reuben JP, Smith AB, Kaczorowski GJ, Garcia ML. Biochemistry 1994;33:5819. [PubMed: 7514038]
6. Selala MI, Daelemans F, Schepens PJC. Drug Chem. Toxicol 1989;12:237. [PubMed: 2698801]
7. Yao Y, Peter AB, Baur R, Sigel E. Mol. Pharmacol 1989;35:319. [PubMed: 2538710]
8. Rabindran SK, Ross DD, Doyle LA, Yang WD, Greenberger LM. Anticancer Res 2000;60:47.
9. Dowd PF, Cole RJ, Vesonder RF. J. Antibiot 1988;41:1868. [PubMed: 3209479]
10. Hayashi H. Recent Res. Dev. Agric. Biol. Chem 1998;2:511.
11. Hayashi H, Asabu Y, Murao S, Nakayama M, Arai M. Chem. Express 1993;8:177.
12. Saikia S, Nicholson MJ, Young C, Parker EJ, Scott B. Mycol. Res 2008;112:184. [PubMed: 18262778]
13. Kato N, Suzuki H, Takagi H, Asami Y, Kakeya H, Uramoto M, Usui T, Takahashi S, Sugimoto Y, Osada H. Chembiochem 2009;10:920. [PubMed: 19226505]
14. Steffan N, Grundmann A, Yin WB, Kremer A, Li SM. Curr. Med. Chem 2009;16:218. [PubMed: 19149573]
15. Ding YS, de Wet JR, Cavalcoli J, Li SY, Greshock TJ, Miller KA, Finefield JM, Sunderhaus JD, McAfoos TJ, Tsukamoto S, Williams RM, Sherman DH. J. Am. Chem. Soc 2010;132:12733. [PubMed: 20722388]
16. Clardy J, Springer JP, Buchi G, Matsuo K, Wightman R. J. Am. Chem. Soc 1975;97:663. [PubMed: 1133368]
17. Ariza MR, Larsen TO, Petersen BO, Duus JO, Barrero AF. J. Agric. Food. Chem 2002;50:6361. [PubMed: 12381117]
18. Frisvad JC, Samson RA. Studies in Mycol 2004:1.
19. Wong SM, Musza LL, Kydd GC, Kullnig R, Gillum AM, Cooper R. J. Antibiot 1993;46:545. [PubMed: 7684734]
20. Takahashi C, Matsushita T, Doi M, Minoura K, Shingu T, Kumeda Y, Numata A. J. Chem. Soc., Perkin Trans 1995;1:2345.
21. Finking R, Marahiel MA. Annu. Rev. Microbiol 2004;58:453. [PubMed: 15487945]
22. Stack D, Neville C, Doyle S. Microbiology-Sgm 2007;153:1297.
23. Ames BD, Walsh CT. Biochemistry 2010;49:3351. [PubMed: 20225828]

24. Ames BD, Liu XY, Walsh CT. Biochemistry 2010;49:8564. [PubMed: 20804163]
25. Jiao RH, Xu S, Liu JY, Ge HM, Ding H, Xu C, Zhu HL, Tan RX. Org. Lett 2006;8:5709. [PubMed: 17134253]
26. Larsen TO, Petersen BO, Duus JO. J. Agric. Food Chem 2001;49:5081. [PubMed: 11600070]
27. Springer JP. Tetrahedron Lett 1979:339.
28. Yamazaki M, Okuyama E. Chem. Pharm. Bull 1979;27:1611. [PubMed: 396046]
29. Chooi YH, Cacho R, Tang Y. Chem. Biol 2010;17:483. [PubMed: 20534346]
30. Yin WB, Grundmann A, Cheng J, Li SM. J. Biol. Chem 2009;284:100. [PubMed: 19001367]
31. Wang S, Xu Y, Maine EA, Wijeratne EM, Espinosa-Artiles P, Gunatilaka AA, Molnar I. Chem. Biol 2008;15:1328. [PubMed: 19101477]
32. Wiest A, Grzegorski D, Xu BW, Goulard C, Rebuffat S, Ebbole DJ, Bodo B, Kenerley C. J. Biol. Chem 2002;277:20862. [PubMed: 11909873]
33. Rausch C, Weber T, Kohlbacher O, Wohlleben W, Huson DH. Nucleic Acids Res 2005;33:5799. [PubMed: 16221976]
34. Sattely ES, Fischbach MA, Walsh CT. Nat. Prod. Rep 2008;25:757. [PubMed: 18663394]
35. Pfeifer BA, Admiraal SJ, Gramajo H, Cane DE, Khosla C. Science 2001;291:1790. [PubMed: 11230695]
36. Kutchan TM, Dittrich H. J. Biol. Chem 1995;270:24475. [PubMed: 7592663]
37. Kawamoto S, Mizuguchi Y, Morimoto K, Aki T, Shigeta S, Yasueda H, Wada T, Suzuki O, Jyo T, Ono K. Biochim. Biophys. Acta 1999;1454:201. [PubMed: 10381565]
38. Fujimoto H, Negishi E, Yamaguchi K, Nishi N, Yamazaki M. Chem. Pharm. Bull 1996;44:1843.
39. Mhaske SB, Argade NP. Tetrahedron 2006;62:9787.
40. van den Berg MA, et al. Nat. Biotechnol 2008;26:1161. [PubMed: 18820685]
41. Fedorova ND, et al. PLos Genet 2008;4
42. Zhang S, Schwelm A, Jin H, Collins LJ, Bradshaw RE. Fungal Genet Biol 2007;44:1342. [PubMed: 17683963]
43. Bruckner H, Becker D, Gams W, Degenkolb T. Chem. Biodivers 2009;6:38. [PubMed: 19180454]
44. Rebuffat S, Duclohier H, Auvin-Guette C, Molle G, Spach G, Bodo B. FEMS Immunol. Microbiol 1992;105:151.
45. Sansom MSP. Prog. Biophys. Mol. Biol 1991;55:139. [PubMed: 1715999]
46. Kubicek CP, Komon-Zelazowska M, Sandor E, Druzhinina IS. Chem. Biodivers 2007;4:1068. [PubMed: 17589877]
47. Daniel JFD, Rodrigues E. Nat. Prod. Rep 2007;24:1128. [PubMed: 17898900]
48. Pojer F, Li SM, Heide L. Microbiology 2002;148:3901. [PubMed: 12480894]
49. Pojer F, Kahlich R, Kammerer B, Li SM, Heide L. J. Biol. Chem 2003;278:30661. [PubMed: 12777382]
50. Raap J, Erkelens K, Ogrel A, Skladnev DA, Bruckner H. J. Pept. Sci 2005;11:331. [PubMed: 15635654]
51. Reiber K, Neuhof T, Ozegowski JH, Von Dohren H, Schwecke T. J. Pept. Sci 2003;9:701. [PubMed: 14658790]
52. Mohr H, Kleinkauf H. Biochim. Biophys. Acta 1978;526:375. [PubMed: 568941]
53. Szewczyk E, Nayak T, Oakley CE, Edgerton H, Xiong Y, Taheri-Talesh N, Osmani SA, Oakley BR. Nat. Protoc 2006;1:3111. [PubMed: 17406574]
54. Pall M, Brunelli J. Fungal Genet. Newsl 1993;40:59.
55. Mullaney EJ, Hamer JE, Roberti KA, Yelton MM, Timberlake WE. Mol. Gen. Genet 1985;199:37. [PubMed: 3158796]
56. Punt PJ, Dingemanse MA, Kuyvenhoven A, Soede RDM, Pouwels PH, Vandenhondel C. Gene 1990;93:101. [PubMed: 2121607]
57. Chooi YH, Stalker DM, Davis MA, Fujii I, Elix JA, Louwhoff S, Lawrie AC. Mycol. Res 2008;112:147. [PubMed: 18280724]

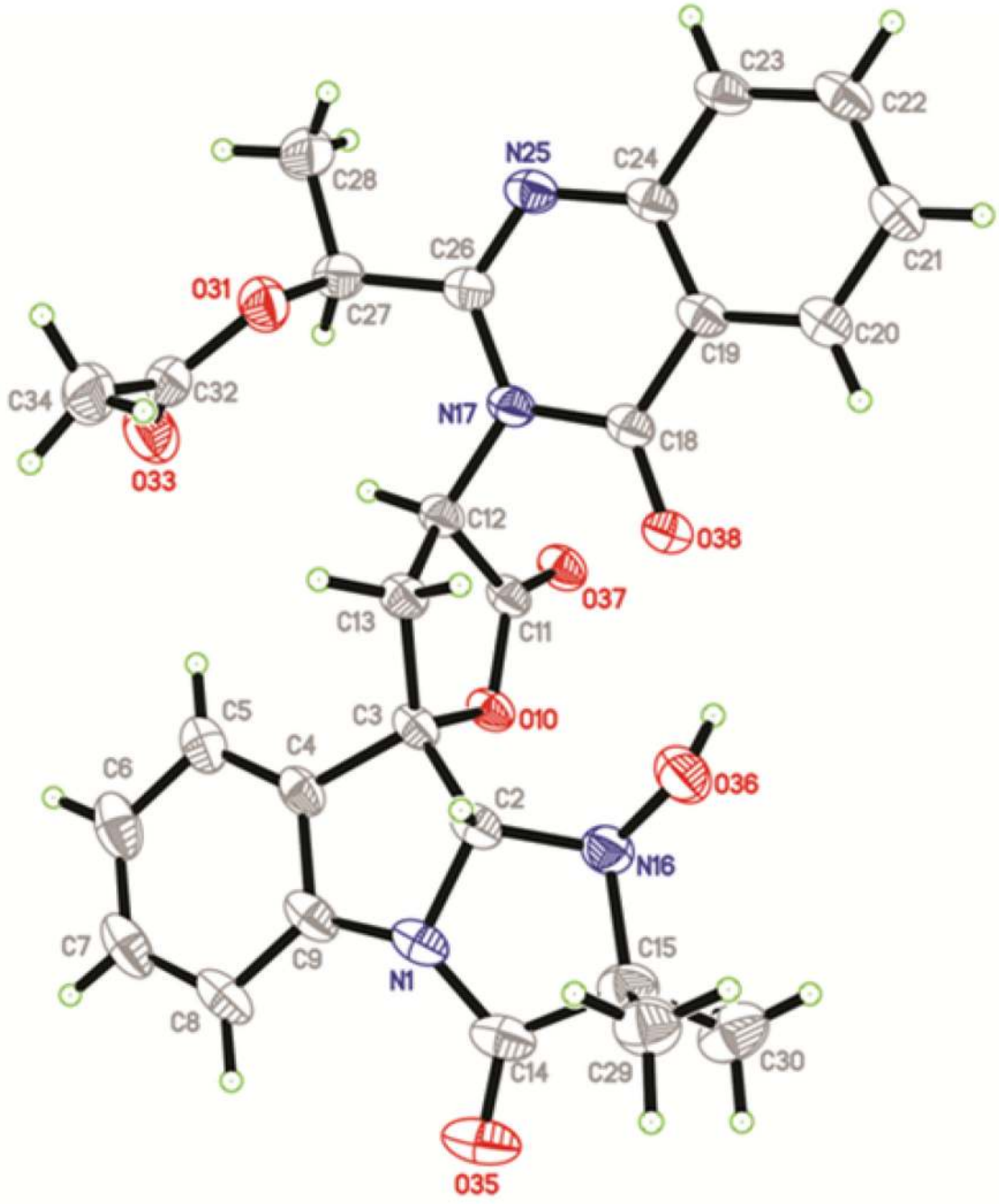

Figure 1.
A perspective drawing of **1**.

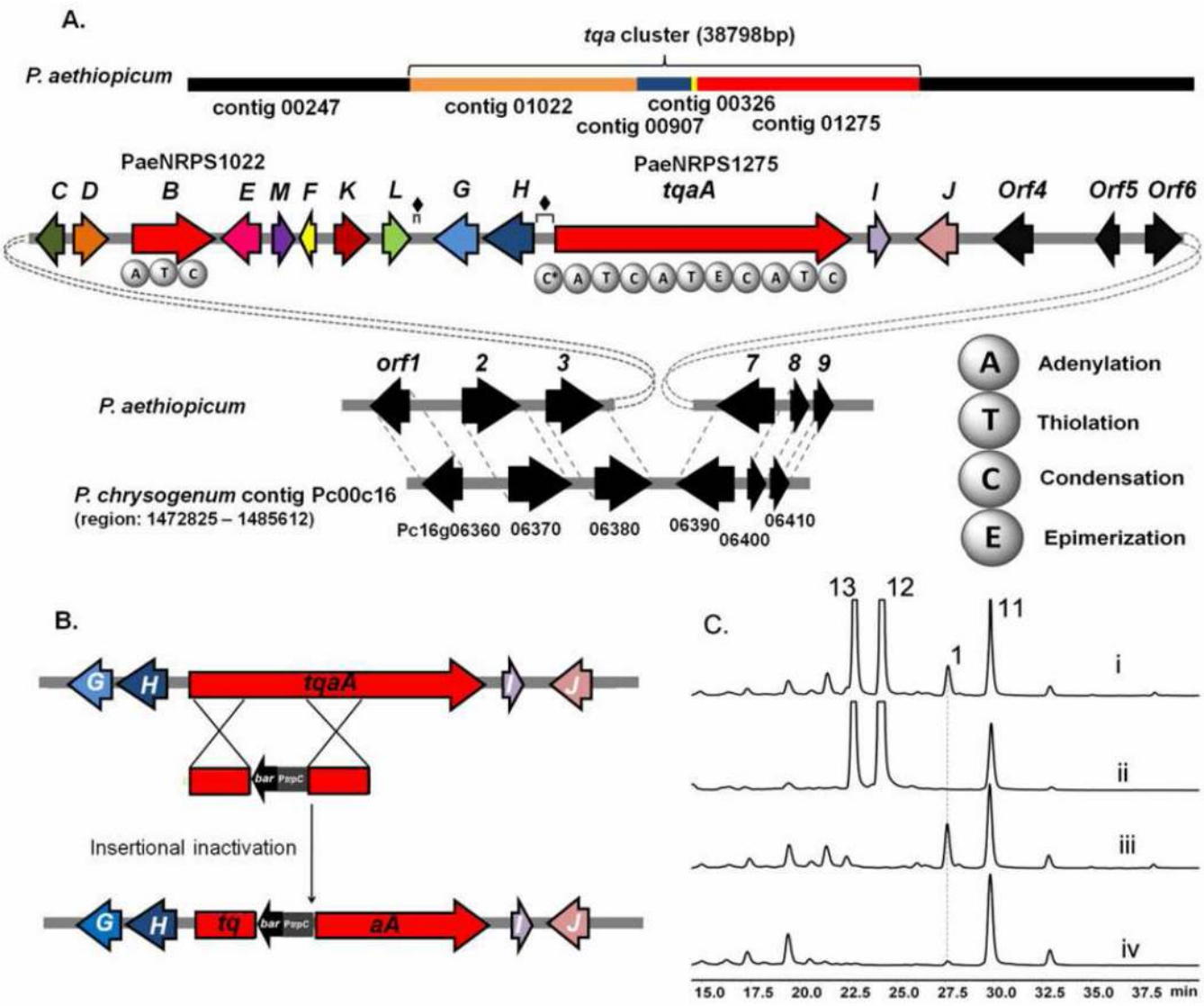

Figure 2.

Organization of the *tqa* gene cluster and genetic verification of involvement in **1** biosynthesis. (A) The *tqa* gene cluster; (B) Knockout strategy used to inactivate *tqaA*; (C)HPLC (280 nm) traces of metabolic extracts from single gene deletion strains of *P. aethiopicum*. Trace i: wild type strain producing **1, 11–13**; trace: ii, Δ*tqaA*; trace iii, Δ*gsfA*. This strain was constructed to eliminate the high titer metabolites **12** and **13**; and trace iv, Δ*gsfA*/Δ*tqaK*. ♦ indicates repeating sequences.

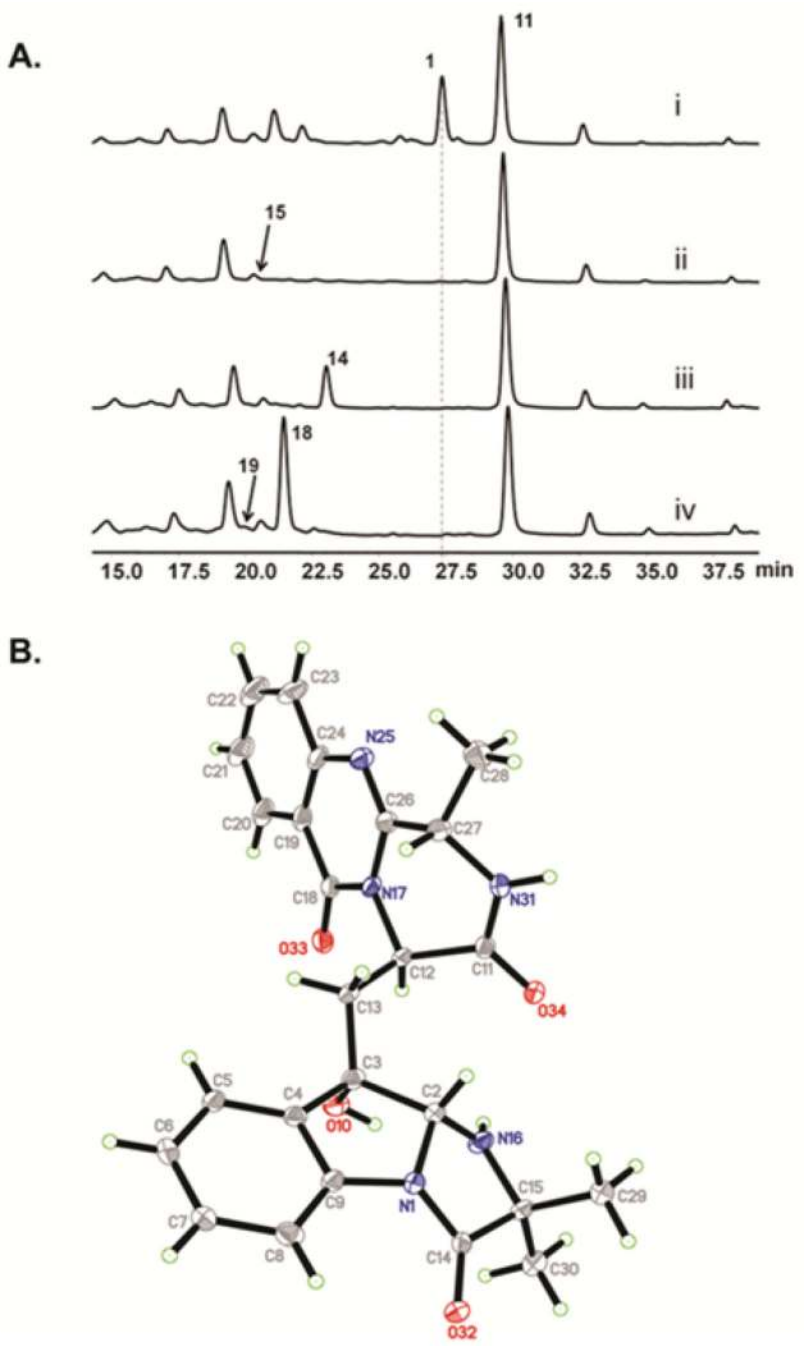

Figure 3.

Biosynthesis of **18** as an intermediate in the *tqa* pathway. (A) HPLC analysis (280 nm) of intermediates accumulated in the knockout strains constructed starting from Δ*gsfA*. Trace i: Δ*gsfA*; trace ii: Δ*gsfA*/Δ*tqaB*; trace iii: Δ*gsfA*/Δ*tqaH*; and trace iv: Δ*gsfA*/Δ*tqaG*. (B) A perspective drawing of **18**.

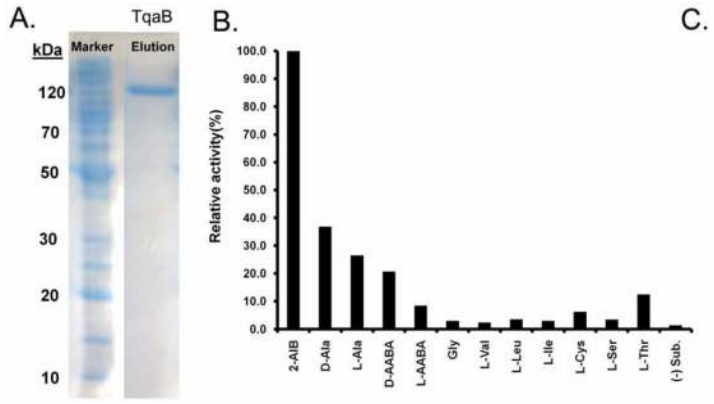

C.

Comparison of the 10 amino acids responsible for Adenylation domains substrate specificity

Name	Pos1[a] (235)	Pos2 (236)	Pos3 (239)	Pos4 (278)	Pos5 (299)	Pos6 (301)	Pos7 (322)	Pos8 (330)	Pos9 (331)	Pos10 (551)
TqaB (U[b])	D	L	F	M	M	C	G	C	I	K
ACLA_017900 (U)	D	L	F	M	M	C	G	C	I	K
AFUA6g012050 (A)	D	L	F	V	L	A	G	C	I	K
Tex1-A1 (U)	D	L	G	Y	L	A	G	V	F	K
Tex1-A5 (U/A)	D	V	F	W	L	C	G	V	F	K
Tex1-A9 (U)	D	L	G	Y	L	A	G	-	C	K
Tex1-A12 (U)	D	L	G	Y	L	A	G	V	F	K
Tex1-A15 (U)	D	L	G	F	L	A	G	V	F	K
Tex1-A16 (U)	D	L	G	F	L	A	G	-	C	K

[a] Residue positions (Pos) are numbered according to GrsA-PheA. [b] Abbreviations: U,2-aminoisobutyric acid; A, alanine.

Figure 4.

Activation of aminoisobutyric acid (AIB) by TqaB. (A) Expression and purification of TqaB from BAP1; (B)ATP-[^{32}P]PP$_i$ exchange assay using purified TqaB (100% relative activity corresponds to 55,000 cpm); (C) Alignment of the specificity-determining residues in TqaB with other related AIB (U)/L-alanine (A) activating domains.

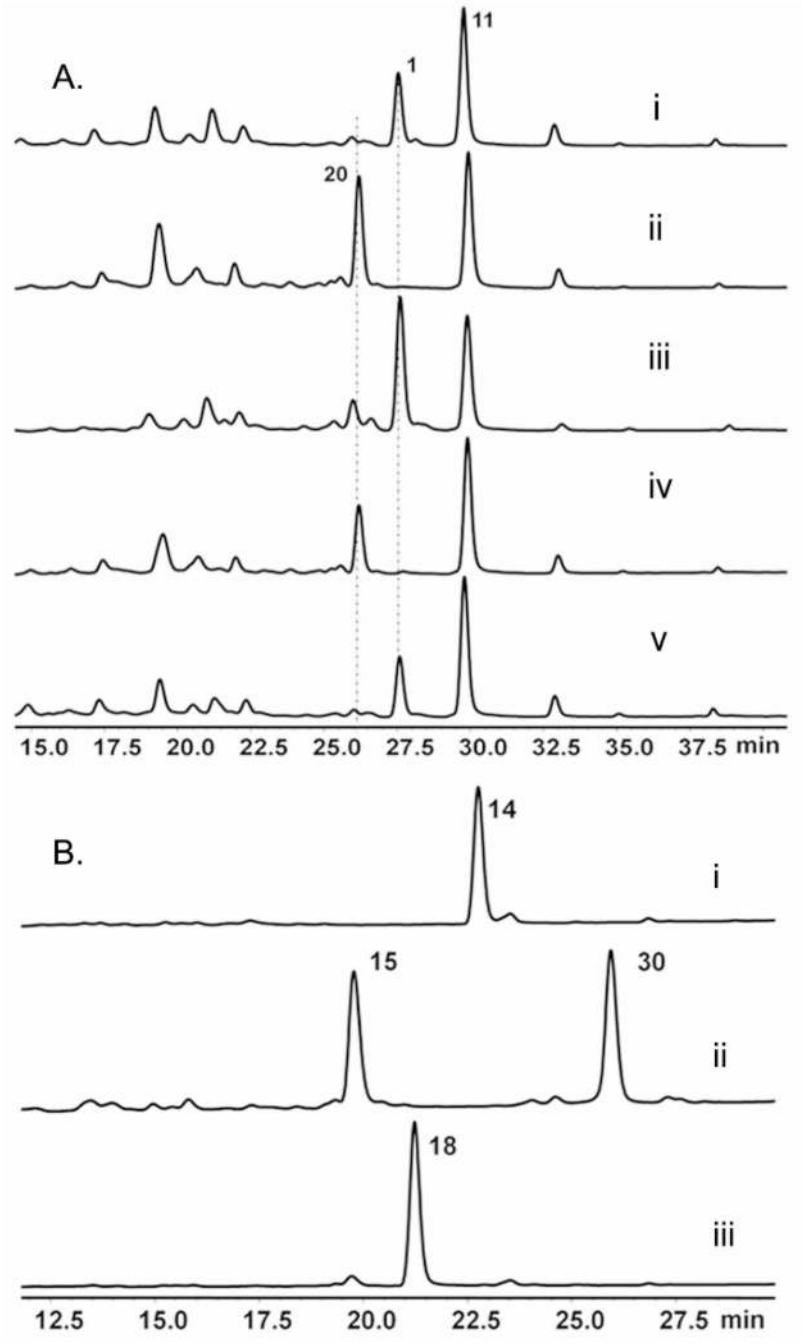

Figure 5.

Identification of *tqa* genes that are likely involved in the biosynthesis of AIB. (A) Extract from the following strains that produced nortryptoquialaine **20** are shown here. Trace i: Δ*gsfA*; trace ii: Δ*gsfA*/Δ*tqaL*; trace iii: Δ*gsfA*/Δ*tqaL* supplied with 1.5 mM AIB; trace iv: Δ*gsfA*/Δ*tqaM*; trace v: Δ*gsfA*/Δ*tqaM* supplied with 1.5 mM AIB demonstrating restoration of biosynthesis of **1**. (B) In vivo feeding of 120 μM **14** to trace i: BAP1 strain (no enzyme overexpression control); trace ii: BAP1 expressing TqaH; and trace iii: BAP1 expressing TqaB and TqaH and supplemented with 1.5 mM AIB.

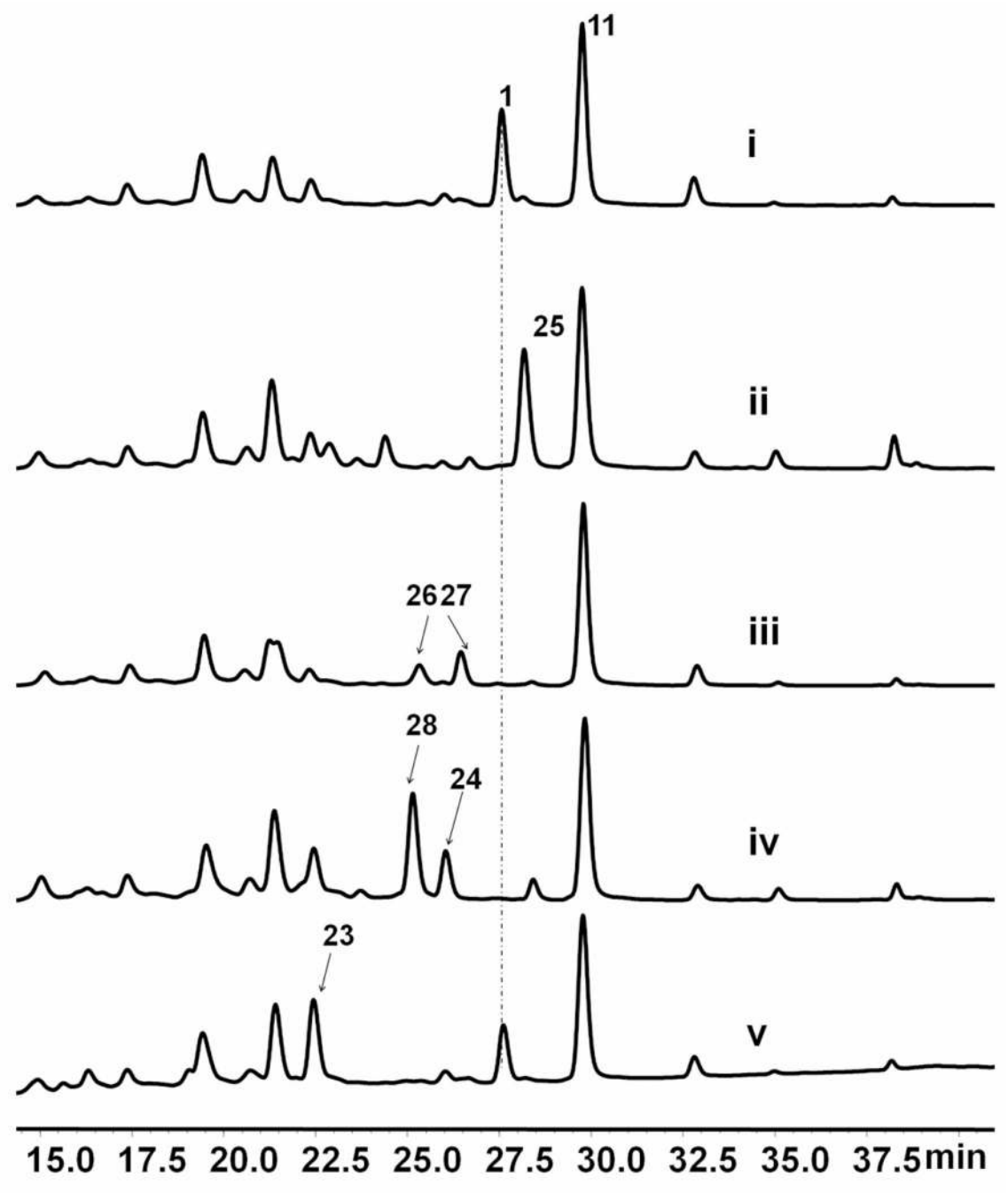

Figure 6.
The remaining steps of **1** biosynthesis as elucidated from the single gene knockout studies. Trace i: Δ*gsfA*; trace ii: Δ*gsfA*/Δ*tqaC*; trace iii: Δ*gsfA*/Δ*tqaD*; trace iv: Δ*gsfA*/Δ*tqaE*; and trace v: Δ*gsfA*/Δ*tqaI*;

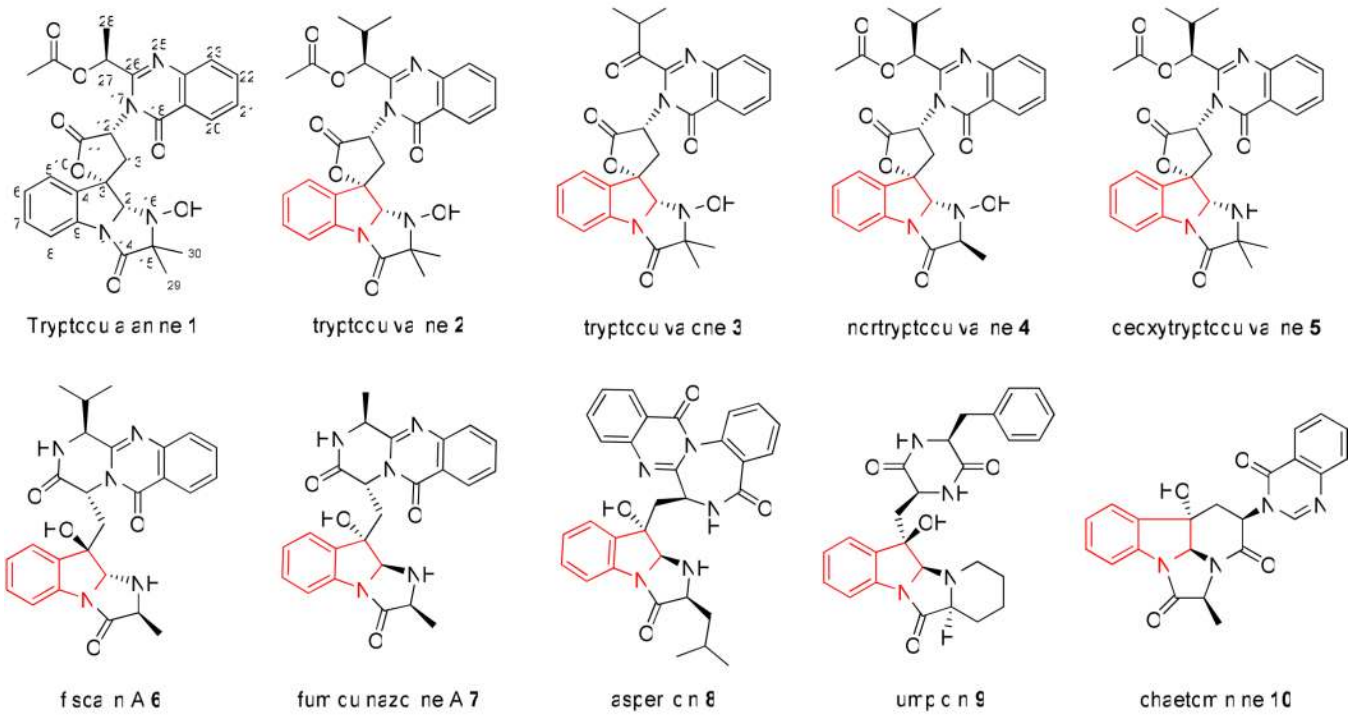

Scheme 1.
Tryptoquialanine **1**, tryptoquivaline **2** and related fungal indole alkaloids

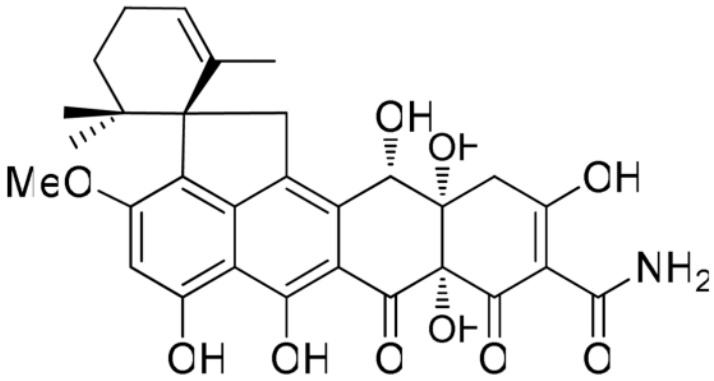

Verrucarin A **11**

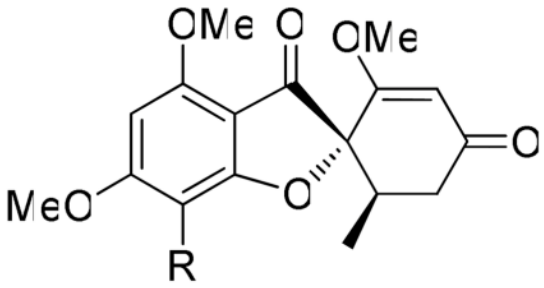

Griseofulvin **12**: R=Cl
Dechlorogriseofulvin **13**: R=H

Scheme 2.
Other metabolites produced by *P. aethiopicum*

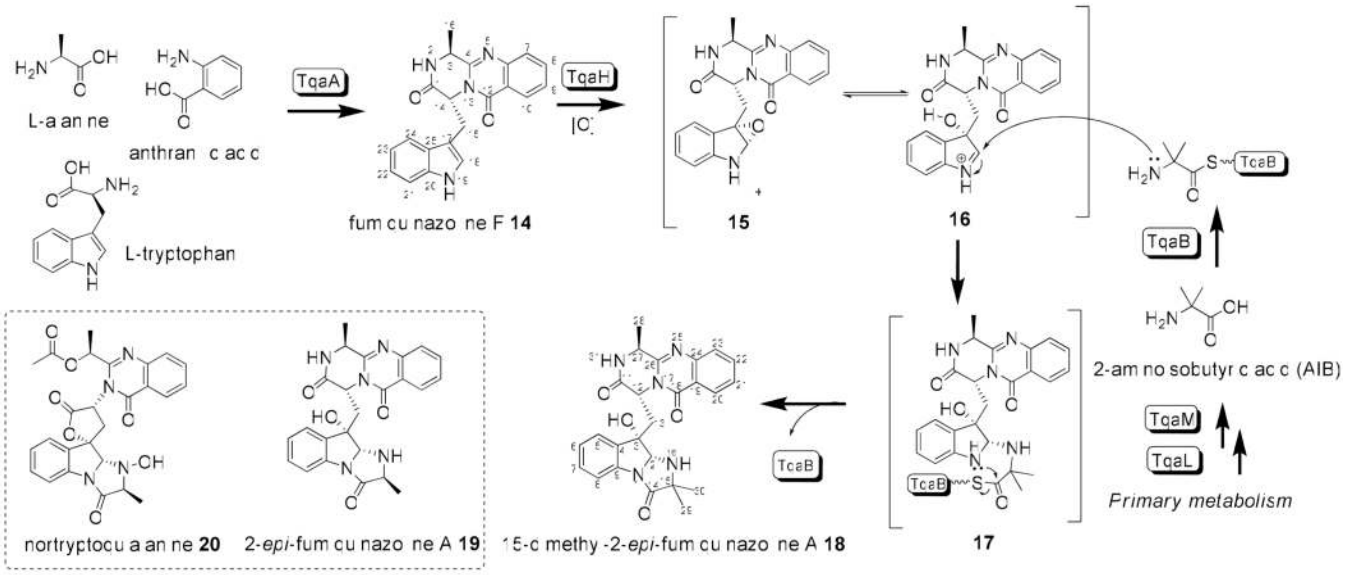

Scheme 3.
Enzymes involved in the synthesis of fumiquinazoline intermediates **14** and **18**

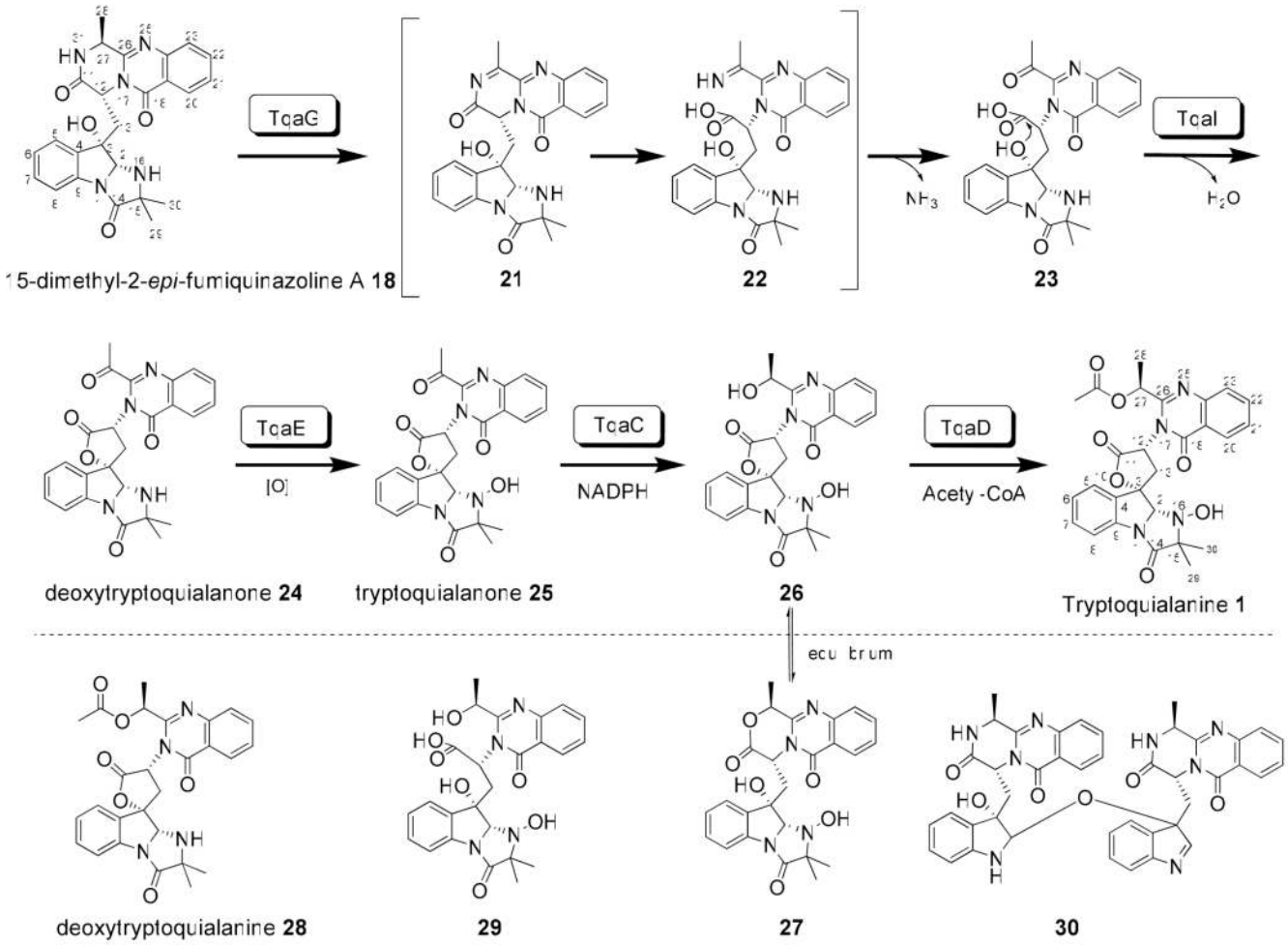

Scheme 4.
Proposed enzymatic steps that convert **18** to **1**

J Am Chem Soc. Author manuscript; available in PMC 2012 March 2.

Table 1

The *tqa* gene cluster and gene functions assignment

Gene	Size (bp/aa)	BLASTP homolog accession number	Identity/ similarity (%)	Putative function	*E*-value	Related metabolite produced after KO
tqaA	12310/4095	ACLA_017890 AFUA_6G12080	64/77 54/69	NRPS (C*ATCATECATC)	0 0	No product
tqaB	3327/1108	ACLA_017900 AFUA_6G12050	67/80 56/72	NRPS (ATC)	0	**15, 30**
tqaC	1106/363	ACLA_061530	59/72	Short-chain dehydrogenase	7e-93	**25**
tqaD	1542/513	ACLA_061540	50/64	Acetyltransferase	2e-113	**26, 27**
tqaE	1620/466	ACLA_017910 ADM34142 *(notI)* ADM34135 *(notB)*	61/73 45/63 43/65	FAD-dependent oxidoreductase	8e-173 2e-101 6e-94	**24, 28**
tqaF	717/238	AO090701000440	70/84	Haloalkanoic acid dehalogenase	4e-98	**1**
tqaG	1723/489	ACLA_017880 AFUA_6G12070	72/83 46/61	FAD-dependent oxidoreductase	0 7e-114	**18, 19**
tqaH	1545/463	ACLA_017920 AFUA_6G12060	65/82 54/70	FAD-dependent oxidoreductase	1e-177 3e-134	**14**
tqaI	810/269	ACLA_017930	54/73	Tryp sin-like serine protease	2e-68	**23**
tqaJ	1852/587	ACLA_098230	55/76	MFS toxin efflux pump	7e-145	**-**
tqaK	1498/416	UREG_02305	33/46	bZIP DNA-binding protein	4e-54	**1**
tqaL	1116/371	NCU01071 ACLA_063370	62/76 60/76	Unknown function	8e-112	**20**
tqaM	1057/311	NCU01072 ACLA_063360	70/82 50/67	Class II aldolase	2e-124 3e-76	**20**
orf4	1302/434	Pc12g07140	96/98	Unknown function	0	**1**
orf5	819/273	PMAA_037110	49/68	RTA1-like transmembrane protein	7e-58	**1**
orf6	1387/417	NECHADRAFT_80860	57/75	Zn2Cys6 transcription factor	3e-74	**1**